

Metal Particle Size in Silica-Supported Copper Catalysts. Influence of the Conditions of Preparation and of Thermal Pretreatments

Thierry Toupance,[†] Maggy Kermarec, and Catherine Louis*

Laboratoire de Réactivité de Surface, UMR 7609 CNRS, Université Pierre et Marie Curie, 4 place Jussieu, F75252 Paris Cedex 05, France

Received: September 22, 1999

The size of metal copper particles supported on silica was studied as a function of the following parameters: the preparation route, the nature of the metallic precursor, the copper content, and the thermal pretreatments before reduction. Two modes of preparation were investigated: (i) incipient wetness impregnation with copper nitrate; (ii) cationic exchange with copper tetraammine and copper bis-ethanediamine complexes. The key step for the obtention of small metal particles after reduction to 700 °C is the drying step at room temperature for the Cu/SiO₂ samples prepared by impregnation and the presence of chemical bonds between Cu²⁺ and the support for the samples prepared by cationic exchange. The chemical bonding is established during drying or calcination, depending on the metal complex. The characterization studies clearly showed that different Cu(II) species (copper nitrate hydroxide, CuO, copper phyllosilicate, or isolated-grafted Cu²⁺ ions) can exist depending on the preparation method and the thermal pretreatment. For the first time, the formation of copper phyllosilicate is pointed out in Cu/SiO₂ samples prepared by cationic exchange.

Introduction

During the first stage of preparation of oxide-supported transition metal catalysts, when the support is in suspension in an aqueous solution containing metal complexes, the latter may interact with the support to form outer-sphere complexes when the metal complexes are in electrostatic interaction with the support, or inner-sphere complexes when they are grafted on the support.^{1,2} Partial dissolution of the support may also occur depending on the solution pH. This may lead to the formation of a supported mixed phase involving the ions of the support and the transition metal ions. This phenomenon of dissolution–precipitation has been extensively studied in the case of the formation of nickel phyllosilicates during the preparation of silica-supported Ni catalysts.³ They are known to form in samples prepared by deposition–precipitation^{4,5} and by cationic exchange with [Ni(NH₃)₆]²⁺.^{6–8}

The subsequent stages of preparation usually involve steps of drying, calcination, and reduction. The understanding of the chemical phenomena occurring during these stages is also of fundamental interest, since, like the nature of the metal–support interaction in solution, they can influence the final state of the catalysts and in particular the size of the metal particles.

This work deals with the preparation of silica-supported copper catalysts. They are usually prepared by impregnation with Cu(NO₃)₂·3H₂O,^{9,10} Cu(acetate)₂·H₂O,^{11–13} or CuCl₂,¹⁴ by cationic exchange with [Cu(NH₃)₄(H₂O)₂]²⁺^{15–19} or [Cu(en)₂(H₂O)₂]²⁺,²⁰ by adsorption of Cu(acac)₂,^{21,22} and by deposition–precipitation of Cu(NO₃)₂·3H₂O.^{10,23–25} Among these studies, only a few on the metal particle sizes have been reported. For samples prepared by impregnation with copper nitrate, Jackson et al.⁹ reported either a bimodal distribution of particle sizes, 60–100 and ~4000 Å, or a single distribution

of large particles, ~4000 Å, depending on the silica support. Kuipjers et al.¹⁰ reported a bimodal distribution in a 25 wt % Cu/SiO₂ catalyst: numerous particles smaller than 200 Å and a small number of very large ones, up to 3000 Å. The copper particle size was also studied by Kohler et al.¹⁹ in materials prepared by cationic exchange with [Cu(NH₃)₄(H₂O)₂]²⁺ and by Geus et al.²³ in materials prepared by deposition–precipitation. In both cases, the average particle size increases with the Cu loading but remains smaller than 40 Å for Cu loadings lower than 10 wt %. No distribution of size was reported.

As such or promoted, the Cu/SiO₂ materials are efficient catalysts for many reactions: hydrogenation of alkynes to alkenes^{25–31} and of ethene to ethane,⁹ selective hydrogenation of α,β -unsaturated carbonyl compounds to their corresponding unsaturated alcohols,³² methanol synthesis from H₂ and CO or CO₂,³³ dehydrogenation of alcohols,^{34–38} hydrogenolysis of esters to their corresponding alcohols.^{17,24,25,39} They are also active for the water gas shift reaction.¹⁰ Often, their catalytic properties including deactivation depend on the size of the metal particles and the metal–support interaction, i.e., on the preparation route of these materials.^{10,17,32,34,37,38} It is therefore important to be able to control the size of the metal particles through the various steps of preparation leading to the activated catalyst.

The aim of this study is to have a better view of the chemical changes undergone by the copper precursor during thermal pretreatments (drying and calcination) to find the key parameters that control the metal particle size. The following parameters are also investigated: the preparation method (impregnation and cationic exchange), the nature of the metal precursor (exchange with copper tetraammine or with copper bis-ethanediamine), and the copper loading. The relevance of the drying step that is usually neglected in the literature is emphasized in this paper. It is shown that it is possible to obtain small metal particles even in samples prepared by impregnation by tuning the parameters of the drying step. The nature and conditions of formation of the different supported copper species before

[†] Present address: Laboratoire de Chimie Organique et Organométallique, UMR 5802 CNRS, Université Bordeaux I, 351 cours de la Libération, F33405 Talence Cedex, France.

reduction (copper nitrate hydroxide, grafted Cu^{2+} , copper phyllosilicate, or copper oxide) are pointed out, and a comparison with the Ni/SiO_2 system is given. For the first time, the formation of copper phyllosilicate is evidenced in Cu/SiO_2 samples prepared by cationic exchange.

Experimental Section

1. Catalyst Preparation. All the samples were prepared with a nonporous silica, Aerosil Degussa 380 ($380 \text{ m}^2 \text{ g}^{-1}$). Commercial copper nitrate ($\text{Cu}(\text{NO}_3)_2 \cdot 3\text{H}_2\text{O}$; 99.999% Aldrich) was used. Two different modes of deposition were investigated: incipient wetness impregnation with copper nitrate; cationic exchange with copper tetraammine and with copper bis-ethanediamine. After drying, some samples were calcined under flowing dry O_2 (200 mL min^{-1}) at 450°C for 15–18 h.

a. Incipient Wetness Impregnation with Copper Nitrate ($\text{Cu}(\text{NO}_3)_2 \cdot 3\text{H}_2\text{O}$). Aqueous solutions with two different concentrations of copper nitrate (0.14 and 0.57 mol L^{-1}) were put into contact with 2 g of silica with an impregnation volume of $3\text{--}3.5 \text{ mL g}^{-1}$. After thorough mixing, a blue gel was obtained. The samples were dried in air either at room temperature or at 100°C for various times and possibly calcined. Samples with 4 and $16 \text{ wt } \%$ of copper were obtained (thereafter referred to as ICu_4 and ICu_{16} , respectively).

b. Cationic Exchange. i. With Copper Tetraammine ($[\text{Cu}(\text{NH}_3)_4(\text{H}_2\text{O})_2]^{2+}$). The samples were prepared from solutions of $\text{Cu}(\text{NH}_3)_4(\text{H}_2\text{O})_2(\text{NO}_3)_2$ (0.025 and 0.2 mol L^{-1}) obtained by mixing a suitable amount of copper nitrate with an excess of ammonia. The pH of the solutions was 11.75 . A volume of 70 mL of solution was poured on 2.5 g of silica, which induced a slight decrease in the pH value (11.25). The suspensions were continuously stirred for 24 h in a closed temperature-controlled vessel at 25°C . The suspensions were then filtered, and the samples were washed four times with 50 mL of distilled water to obtain clear solutions. The samples were dried at 100°C and possibly calcined. Samples with 4.5 and $11 \text{ wt } \%$ of copper were obtained (thereafter referred to as $\text{ECu}_{\text{am}}4$ and $\text{ECu}_{\text{am}}11$, respectively).

ii With Copper Bis-ethanediamine ($[\text{Cu}(\text{en})_2(\text{H}_2\text{O})_2]^{2+}$). This sample was prepared from a solution of $\text{Cu}(\text{en})_2(\text{H}_2\text{O})_2(\text{NO}_3)_2$ (0.2 mol L^{-1}) obtained by mixing a solution of copper nitrate with a small excess of ethanediamine (2.2 equiv). The pH of the solution was 11.5 . A volume of 70 mL of solution was poured on 2.5 g of silica, and the pH decreased to 9.5 . The suspension was continuously stirred for 64 h in a closed temperature-controlled vessel at 25°C . The suspension was then filtered and washed as described above. The sample was dried at 100°C and possibly calcined. A sample with $2.2 \text{ wt } \%$ of copper was obtained (thereafter referred to as $\text{ECu}_{\text{en}}2$).

c. Bulk Chrysocolla. Bulk chrysocolla, synthesized by A. Decarreau (HydrASA, URA 721 CNRS, Université de Poitiers, France) according to a hydrothermal process described in ref 40, was used as a reference for the characterization of the Cu/SiO_2 samples.

2. Techniques. Chemical analyses of copper were performed at the Center of Chemical Analysis of the CNRS (Vernaison, France). The Cu weight loading of the samples is expressed in wt % of Cu per gram of sample calcined at 1000°C :

$$\text{wt } \% \text{ Cu} = \frac{m_{\text{Cu}}}{m_{\text{CuO}} + m_{\text{SiO}_2}} \times 100$$

UV–visible–NIR spectra ($200\text{--}1200 \text{ nm}$) were carried out on a Cary 5E spectrophotometer equipped with a Cary 4/5

diffuse reflection sphere. The baseline was recorded using a poly(tetrafluoroethylene) reference. The strong absorptions between 200 and 300 nm are due to ligand–metal charge-transfer bands from O^{2-} of silica to Si^{4+} and from ligands to Cu^{2+} .⁴¹ The main absorption band observed in the $\sim 600\text{--}800 \text{ nm}$ range corresponds to the d–d transition bands of Cu^{2+} . The free Cu^{2+} ion (d^9) has a single spectral term 2D with five degenerate d orbitals. In an O_h symmetry complex, the crystal field due to the ligands induces a splitting of these orbitals into two new energy levels, e_g and t_{2g} , leading to a single d–d transition $^2E_g \rightarrow ^2T_{2g}$ in the visible range. Because of the Jahn–Teller effect, the symmetry of the Cu^{2+} complexes is lowered, i.e., square-planar or octahedral with tetragonal distortion (D_{4h}). The e_g and t_{2g} energy levels are split into two sublevels b_{1g} and a_{1g} , and b_{2g} and e_g , respectively, leading to three d–d transition bands. The broad d–d transition band experimentally observed for the Cu^{2+} complexes is the envelope of these three transition bands.

The X-ray diffraction (XRD) patterns were recorded on a Siemens diffractometer (D500) using $\text{Cu K}\alpha$ radiation. The phase identifications were performed by comparison with the tabulated Joint Committee on Powder Diffraction Standards (JCPDS) d spacing files.

For the IR studies, the samples were finely ground and dispersed into KBr pellets. The IR spectra were scanned at room temperature using a Bruker FTIR IFS 66V spectrometer equipped with a DTGS detector. The spectral resolution was 4 cm^{-1} , and 20 scans were recorded for each spectrum.

The electron spin resonance (ESR) measurements were performed at room temperature and at 77 K on a Bruker ESP300E spectrometer operating in X band (9.3 GHz). Standard 100 MHz field modulation, 10 G amplitude modulation, and 10 mW microwave power were used.

The samples were reduced by temperature-programmed reduction (TPR) from room temperature to 700°C with a heating rate of $7.5^\circ\text{C min}^{-1}$ and under $5\% \text{ v/v H}_2$ in argon (25 mL min^{-1}) at atmospheric pressure.

The average size of the metal copper particles obtained after reduction was measured from the electron micrographs obtained by transmission electron microscopy (TEM, JEOL 100 CXII). Depending on the samples, 350 to more than 1000 particles were counted. The average particle diameter was inferred from the following formula: $d_m = \sum n_i d_i / \sum n_i$, where n_i is the number of particles of diameter d_i . The detection limit of the particles is $\sim 10 \text{ \AA}$. The particles smaller than $70\text{--}100 \text{ \AA}$ were observed on micrographs obtained with a magnification of $160\,000$ or $230\,000$. The large particles were observed at lower magnification. When the distribution of the size of metal particles was found to be bimodal, the average size of the small ($< 100 \text{ \AA}$) and of the large metal particles ($> 100 \text{ \AA}$) was given separately. The ratio of the number of particles of each range was not determined.

Results

I. Cu/SiO_2 Samples Prepared by Impregnation. 1. Dried ICu Samples. No diffraction lines are visible for the ICu_{16} sample dried at room temperature. In contrast, a diffraction pattern is clearly visible when ICu_{16} is dried at 100°C for 24 or 96 h (Figure 1a) and only visible as traces after drying for 3 h . The diffraction pattern does not correspond to that of copper nitrate (Figure 1b) but to that of a copper nitrate hydroxide $\text{Cu}_2(\text{OH})_3(\text{NO}_3)$ (Figure 1c,d). The change in color of the ICu_{16} samples during drying, from blue to green-blue, is also consistent

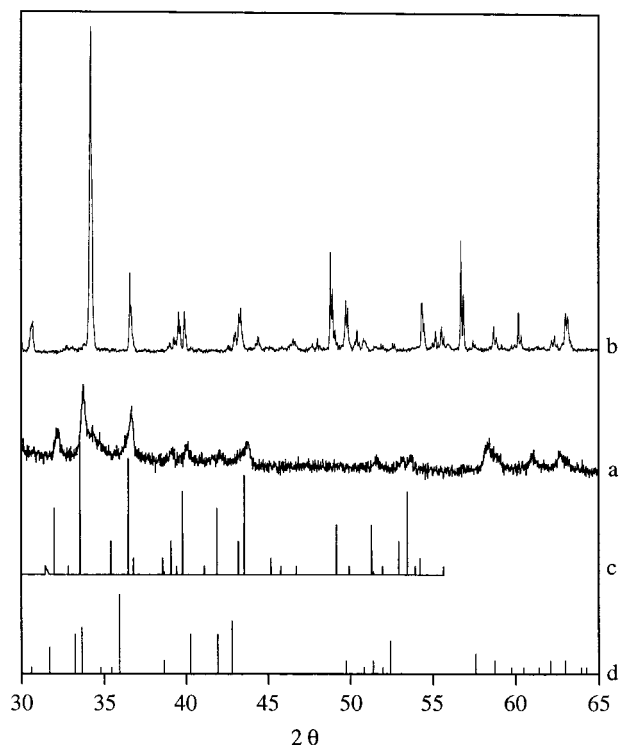


Figure 1. XRD spectra of (a) ICu16 dried at 100 °C/96 h, (b) Cu(NO₃)₂·3H₂O used for the preparations, (c) Cu₂(OH)₃(NO₃) JCPDS file 450594, (d) Cu₂(OH)₃(NO₃) JCPDS file 150014.

with the nitrate transformation into nitrate hydroxide, since the latter is green. As for the ICu4 samples, they remain blue even after prolonged drying at 100 °C. No diffraction lines are observed except for the sample dried at 100 °C/96 h, but they are as weak as for ICu16 dried at 100 °C/3 h.

The UV–visible–NIR spectra (Figure 2 and Table 1) show that the Cu²⁺ d–d transition band of the ICu4 and ICu16 samples shifts to the blue from 800 to ~730 nm when the temperature and the drying time at 100 °C increase. Almost the same shift, from 820 to 750 nm, is observed when a mechanical mixture of copper nitrate and silica (16 wt % of Cu in silica) is heated at 100 °C in air for 96 h. During this treatment, copper nitrate also transforms into copper nitrate hydroxide as indicated by the XRD pattern that is similar to that of Figure 1a. Hence, the blue shift to ~730 nm indicates a change in the environment of the Cu²⁺ ions during the drying step at 100 °C and is consistent with the gradual transformation of the copper nitrate into copper nitrate hydroxide when drying at 100 °C is prolonged.

The electron spin resonance (ESR) spectra of the dried ICu samples recorded at 77 K show an axial signal ($g \approx 2$) of Cu²⁺ ions broadened by magnetic interaction (spectra not shown). The hyperfine structure ($I = 3/2$ for ⁶³Cu and ⁶⁵Cu with 100% natural abundance) is not resolved. A signal at half-field at $g \approx 4.2$ is also observed, indicating the presence of dinuclear or polynuclear Cu^{II} species.^{42,43} The ESR spectra therefore indicate the presence of Cu²⁺ ions interacting with each other.

2. Calcined ICu Samples. After calcination at 450 °C, all the ICu16 samples are gray-black and exhibit a diffraction pattern similar to that of bulk CuO (diffractograms not shown). The diffraction lines are more intense for the samples dried at 100 °C than for that dried at 25 °C (the surface area of the diffraction lines is 50% higher), while the line widths do not change and correspond to coherence domains of 230 Å (calculated from the full width at half-maximum (fwhm) of the (110) and (−202)

lines). This result allows us to deduce that when the sample is dried at 25 °C, all of the copper is not transformed into CuO or a population of CuO particles is not visible because they are too small and/or amorphous. Concerning the ICu4 samples, only ICu4 dried at 100 °C/96 h exhibits a diffraction pattern characteristic of CuO. The other samples do not diffract. Their colors are different too; the ICu4 sample dried at 100 °C/96 h is gray, whereas the others are green.

The presence of bulk CuO is confirmed by UV–visible spectroscopy. Indeed, the calcined ICu16 dried at 100 °C/(24 and 96 h) and ICu4 dried at 100 °C/96 h (curves g and h of Figure 2B and curve h of Figure 2A) show an absorption band with a sharp edge and a threshold at 900 nm. The same feature was observed in bulk CuO⁴⁴ and in CuO mixed with alumina.⁴⁵ Copper oxide is a semiconductor, and the threshold at 900 nm corresponds to the energy of the band gap ($E_g = 1.4$ eV). The edge is less sharp in calcined ICu16 dried at 25 or 100 °C/3 h (curves e and f of Figure 2B) probably because the broad Cu²⁺ d–d band at ~760 nm that is observed in the green calcined ICu4 samples (curves e–g of Figure 2A) is superimposed to the edge in these samples. These UV–visible results confirm that in the green calcined ICu4 samples, CuO is not present and that in ICu16 dried at 25 °C and ICu16 dried at 100 °C/3 h all the supported Cu(II) phase is not transformed into CuO, which agrees with the XRD results.

3. Metal Particle Size in the Reduced ICu Samples. Influence of the Thermal Pretreatment. *a. ICu Samples Reduced Directly after Drying.* Copper in the samples reduced by TPR up to 700 °C is probably fully reduced to Cu⁰, since no signal of the Cu²⁺ and Cu⁺ species are observed by ESR and photoluminescence, respectively.

The electron micrographs of the 25 °C-dried reduced ICu samples show numerous small metal particles whose mean size does not seem to depend on the Cu loading: 27 and 34 Å for the 4 and 16 wt % samples, respectively. However, the size distribution is different; it is twice larger in ICu16 than in ICu4 (Table 1). When the samples are dried at 100 °C, larger particles (>100 Å) appear (Table 1), but after a drying time that depends on the Cu loading. They are visible after 3 h of drying in ICu16 and after 96 h in ICu4. The particles can reach ~900 Å in ICu16 but only ~300 Å in ICu4.

b. ICu Samples Reduced after Calcination. When the samples are calcined at 450 °C prior to reduction, the size of the metal particles in the ICu4 samples (Table 1) still depends on the initial drying step despite the fact that calcination is performed at much higher temperature than drying. Indeed, like the samples reduced after drying, the ICu4 samples dried at 25 °C and 100 °C for 3 h contain small metal particles only, with almost the same average size. However, the size distribution is broader for the sample dried at 100 °C/3 h. When the ICu4 sample is dried longer (24 and 96 h), large particles are observed.

The results are different for the ICu16 samples. They all contain large metal particles when they are calcined prior to reduction (Table 1).

II. Cu/SiO₂ Samples Prepared by Cationic Exchange. 1.

ECu_{am} Samples. a. Dried ECu_{am} Samples. As mentioned in the Introduction, we have attempted to detect by FTIR the presence of copper phyllosilicate in the samples prepared by cationic exchange. Copper phyllosilicate, Cu₂Si₂O₅(OH)₂, also called chrysocolla, consists of alternate layers of SiO₄ tetrahedra and discontinuous layers of CuO₆ octahedra^{46,47} (Figure 3). The IR spectrum is characterized by a ν_{SiO} vibration band of SiO₄ tetrahedra at 1023 cm^{−1} and by a δ_{OH} band of the structural hydroxyl groups at 673 cm^{−1}⁴⁶ (Figure 4a).

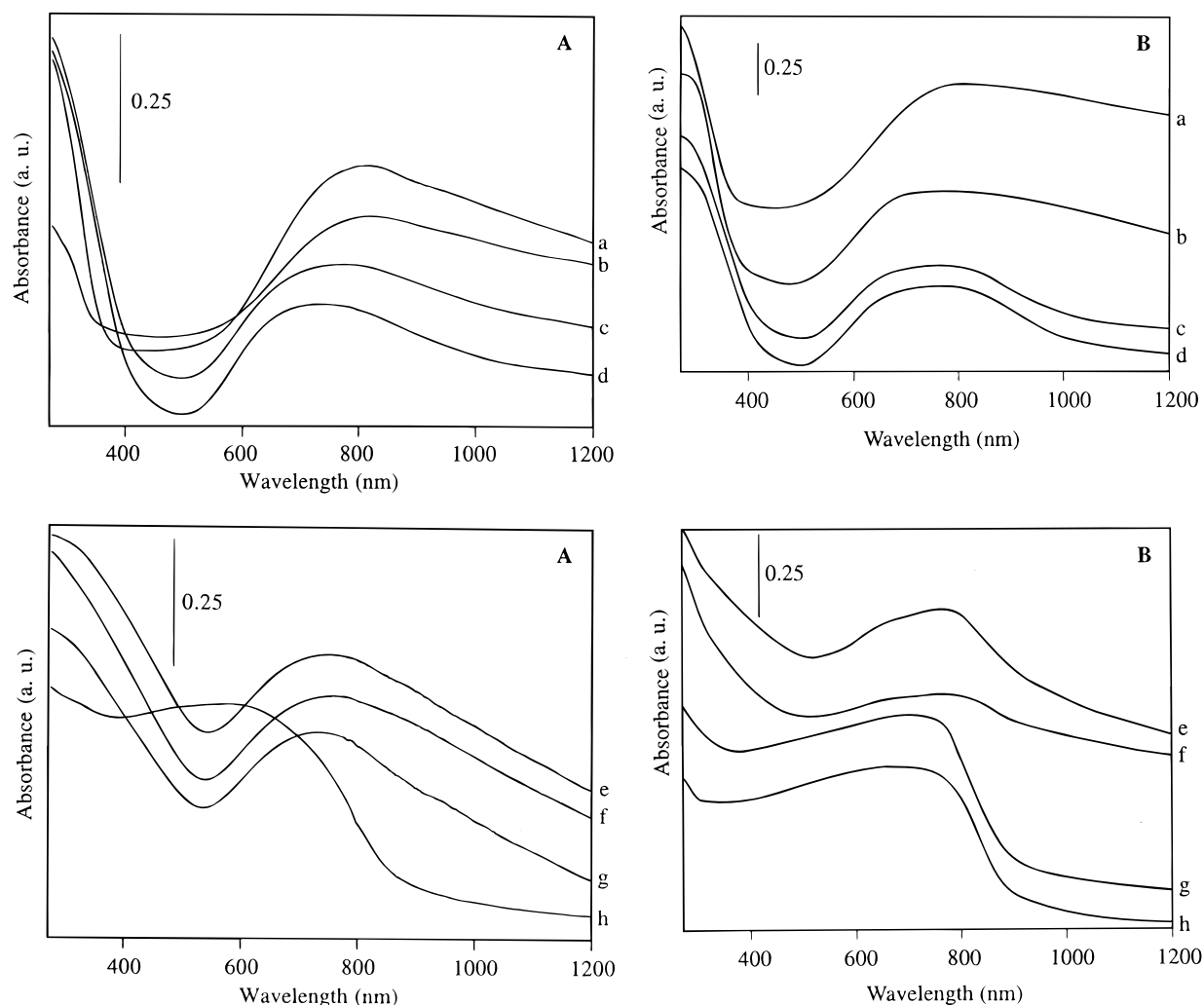


Figure 2. UV-visible-NIR diffuse reflectance spectra of (A) ICu4 and (B) ICu16 dried at (a) 25 °C, (b) 100 °C/3 h, (c) 100 °C/24 h, (d) 100 °C/96 h, (e) 25 °C/calced 450 °C, (f) 100 °C/3 h/calced 450 °C, (g) 100 °C/24 h/calced 450 °C, (h) 100 °C/96 h/calced 450 °C.

TABLE 1: Metal Particle Size in the Impregnated Cu/SiO₂ Samples

sample	pretreatment	“small” particles (<100 Å)		“large” particles (>100 Å)	
		d_{average} (Å)	size distribution (Å)	d_{average} (Å)	size distribution (Å)
ICu4	25 °C	27	10–58		
	100 °C/3 h	27	15–48		
	100 °C/24 h	25	15–55		
	100 °C/96 h	30	15–50	169	50–330
ICu4	25 °C/calced 450 °C	30	14–62		
	100 °C/3 h/calced 450 °C	26	10–90		
	100 °C/24 h/calced 450 °C	27	10–100	383	100–1025
	100 °C/96 h/calced 450 °C	32	15–85	397	106–802
ICu16	25 °C	34	14–110		
	100 °C/3 h	46	14–86	250	100–715
	100 °C/24 h	52	13–100	280	100–845
	100 °C/96 h	33	15–100	229	100–815
ICu16	25 °C/calced 450 °C	34	14–62	470	215–635
	100 °C/3 h/calced 450 °C	31	15–100	399	100–914
	100 °C/24 h/calced 450 °C	34	21–67	310	100–791
	100 °C/96 h/calced 450 °C	35	12–99	251	101–779

In addition to the bands of amorphous silica at about 1100, 800, and 470 cm^{-1} , the IR spectrum of the dried ECu_{am} samples exhibits a shoulder at 1042 cm^{-1} and a band at 671 cm^{-1} (Figure 4c), indicating the formation of a supported chrysocolla phase. The band at 1042 cm^{-1} corresponds to the ν_{SiO} vibration of the supported chrysocolla, since it is observed at 1018 cm^{-1} after subtraction of the spectrum of a silica sample treated under the same conditions of pH and time of contact as in the preparation

of the ECu_{am} sample (spectrum not shown). It may be noted that whatever the copper content and the drying conditions, the FTIR spectra of the ICu samples do not reveal the presence of copper phyllosilicate.

Bulk chrysocolla shows a broad ESR signal between 0 and 8000 G (Figure 5a). The same signal is observed in the dried ECu_{am} samples, but a much thinner and stronger signal is superimposed at $g \approx 2$ (Figure 5c). According to a separate

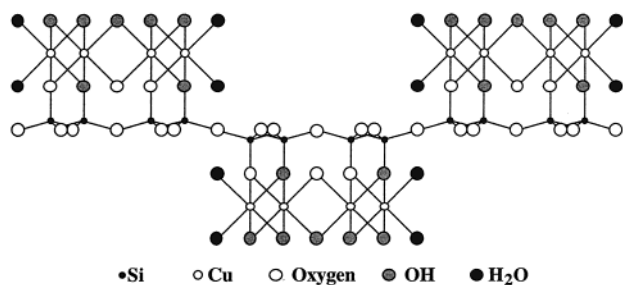


Figure 3. Schematic representation of the structure of natural bulk chrysocolla (according to ref 47).

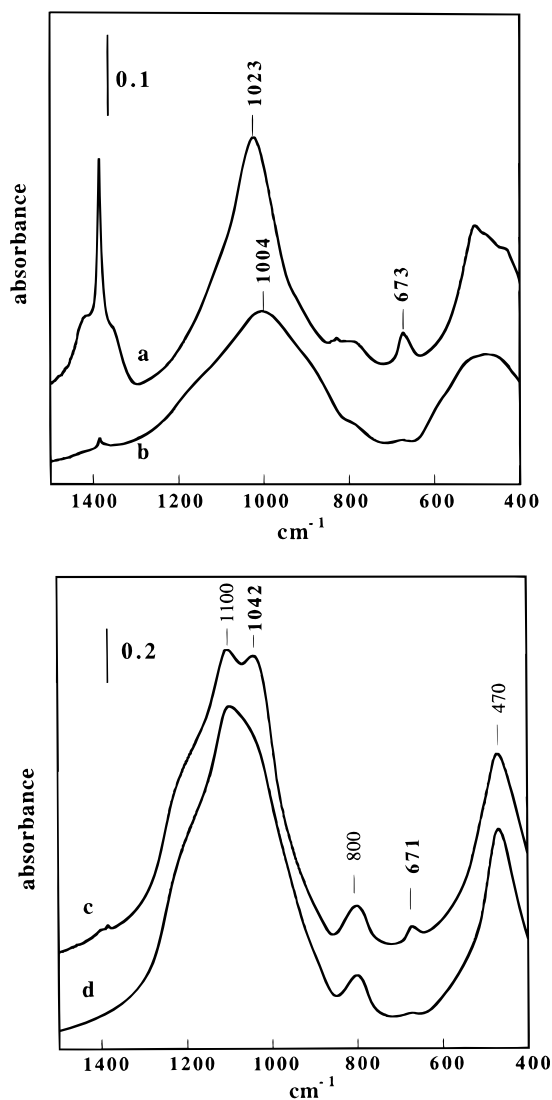


Figure 4. IR spectra of (a) bulk chrysocolla, (b) chrysocolla calcined at 450 °C, (c) ECU_{am}11 dried at 100 °C/64 h, and (d) ECU_{am}11 dried at 100 °C/64 h/calcined 450 °C.

ESR study,⁴⁸ this thin signal is attributed to isolated Cu²⁺ species grafted on the silica surface: $(\equiv\text{SiO})_2\text{Cu}(\text{NH}_3)_2(\text{H}_2\text{O})_2$. This inner-sphere complex was shown to form during the drying step at 25 °C.

b. Calcined ECU_{am} Samples. After calcination at 450 °C, bulk chrysocolla is partially decomposed into silica and CuO. The ν_{SiO} band at 1023 cm⁻¹ has shifted to 1004 cm⁻¹ and broadened, while the δ_{OH} band at 670 cm⁻¹ has strongly decreased in intensity (Figure 4b). The presence of CuO is attested by the XRD pattern (not shown). The intensity of the broad ESR signal

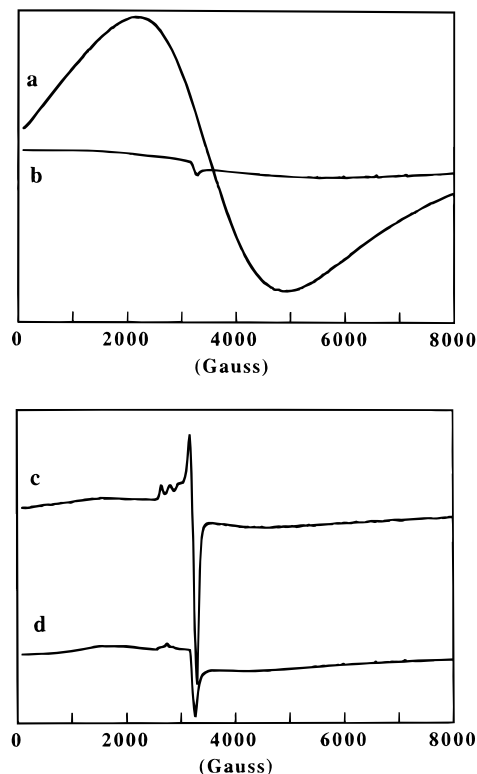


Figure 5. ESR spectra recorded at 77 K of (a) bulk chrysocolla, (b) chrysocolla calcined at 450 °C, (c) ECU_{am}11 dried at 100 °C/64 h, and (d) ECU_{am}11 dried at 100 °C/64 h/calcined 450 °C.

has drastically decreased, and a weak signal at $g = 2$ is visible (Figure 5b), confirming the decomposition of the chrysocolla.

In the case of the ECU_{am} samples calcined at 450 °C, a decrease in the intensity of the IR bands at 1042 and ~ 670 cm⁻¹ is observed (Figure 4d). The ESR spectrum still shows the broad signal of chrysocolla and the thin one (Figure 5d), and the XRD pattern does not show the presence of CuO. The sample is bronze-green and not black as for the calcined chrysocolla. Hence, chrysocolla in the ECU_{am} samples does not seem to fully decompose at 450 °C, as if the presence of the support had a stabilizing effect on this compound.

2. ECU_{en} Samples. Former ESR and UV-visible spectroscopic studies of the ECU_{en} samples^{20,48} have shown that after drying at 25 °C, the supported Cu²⁺ species is $[\text{Cu}(\text{en})_2(\text{H}_2\text{O})_2]^{2+}$ in electrostatic interaction with the silica support. Upon calcination at 450 °C, the ethanediamine ligands are decomposed, and the Cu²⁺ species are grafted on the silica surface as $(\equiv\text{SiO})_2\text{Cu}(\text{H}_2\text{O})_4$. The presence of copper phyllosilicate is not detected by ESR or IR spectroscopies in these samples whether they are dried or calcined.

3. Metal Particle Size in the Reduced ECU Samples. The electron micrographs of the ECU_{am} samples reduced by TPR up to 700 °C exhibit only small metal particles whatever the Cu loading and whether the samples are calcined or not before reduction (Table 2).

In contrast, strong differences in the particle sizes are observed in the ECU_{en} sample depending on whether it is reduced after drying or after calcination. Large metal particles (up to ~ 700 Å) are obtained in the dried sample, whereas only small metal particle sizes (~ 26 Å) with a narrow particle size distribution (14–49 Å) are observed in the calcined sample (Table 2).

In contrast to the impregnated Cu/SiO₂ samples, no large metal particles are formed when the Cu/SiO₂ samples prepared

TABLE 2: Metal Particle Size in the Exchanged Cu/SiO₂ Samples

sample	pretreatment	d_{average} (Å)	size distribution (Å)
ECu _{am} 4	100 °C/96 h	40	13–90
	100 °C/96 h/calcined 450 °C	46	17–106
ECu _{am} 11	100 °C/64 h	43	16–118
	100 °C/64 h/calcined 450 °C	43	15–155
ECu _{en} 2	100 °C/96 h	237	64–687
	100 °C/96 h/calcined 450 °C	26	14–49

by cationic exchange are extensively dried at 100 °C and calcined prior to reduction. Hence, the calcination pretreatment that was detrimental for the formation of small metal particles in impregnated Cu/SiO₂ samples is not detrimental for the exchanged Cu/SiO₂ samples. It may even be advantageous in the case of the ECu_{en} samples, since calcination prevents the formation of the large metal particles that are obtained when the samples are reduced directly after drying (Table 2).

Discussion

1. Cu/SiO₂ Samples Prepared by Impregnation. The influence of the drying conditions on the size of metal particles in Cu/SiO₂ samples prepared by impregnation is emphasized by our results, whether the samples are calcined or not before reduction.

a. ICu Samples Reduced Directly after Drying. The samples reduced without previous calcination may be classified as follows: (i) those dried at 25 °C, which give rise to small metal particles after reduction, whatever the Cu loading; (ii) those dried at 100 °C, which may give rise to large metal particles after reduction, depending on the Cu loading.

The samples dried at 25 °C, i.e., containing copper nitrate, give rise to small metal particles only. It is likely that these small metal particles arise from the reduction of an amorphous phase of hydrated copper nitrate widely spread on the silica surface.

When the samples are dried in air at 100 °C, the XRD patterns reveal the presence of copper nitrate hydroxide (Figure 1), indicating a gradual transformation of the amorphous nitrate into crystalline copper nitrate hydroxide. This transformation is already visible after a 3 h drying of the ICu16 sample, and the diffraction pattern becomes more intense as the drying treatment proceeds (Figure 1a). In addition, TGA experiments⁹ showed that copper nitrate loses water below 100 °C and decomposes into nitrate hydroxide between 100 and 150 °C. After drying at 100 °C for 96 h, the mean size of the particles of nitrate hydroxide calculated from the fwhm of the (200) line is 320 Å. These large particles probably result from the migration and aggregation of the copper nitrate particles during their dehydration/chemical transformation. Therefore, the coexistence of small and large metal particles in the samples dried at 100 °C and then reduced is proposed to arise from the reduction of small particles of amorphous copper nitrate and of large particles of copper nitrate hydroxide, respectively. Hence, as already observed several times in other systems,^{49,50} the metal particle size is directly dependent on the nature and size of the precursor particles.

For the low-loaded ICu4 samples, copper aggregation probably occurs to a lesser extent, since only weak and broad diffraction lines of copper nitrate hydroxide are observed after 96 h of drying. The pattern is similar to that of ICu16 dried at 100 °C/3 h (XRD patterns not shown). This is probably due to the higher spreading of the starting Cu nitrate, which leads to smaller particles of copper nitrate hydroxide.

It can be noted that the influence of the drying step (temperature and duration) on the size of metal particles has been completely neglected in the previous studies on impregnated Cu/SiO₂ samples.^{9,10} More generally speaking, this step is usually neglected in the preparation of supported catalysts, and samples are usually dried in air at ~100 °C without special care. In contrast to the published results (see Introduction), our results show that it is possible to obtain small metal particles in impregnated Cu/SiO₂ samples and that the key step to generate small metal particles is to dry the samples at room temperature.

b. ICu Samples Reduced after Calcination. Depending on the Cu loading, calcination may also have an influence on the metal particle size. It has little effect in the ICu4 samples as long as the samples are dried at 25 or 100 °C for 3 h; average sizes of ~30 Å are found whether the samples are calcined or not prior to reduction, but the size distribution is broader when they are calcined (Table 1). Calcined ICu4 dried at 100 °C/96 h gives small and large metal particles with a broader distribution than when it is reduced directly after drying. It may be recalled that this sample is the only one of the set to show CuO by XRD and UV–visible spectroscopy after calcination (curve h of Figure 2A).

Whatever the drying conditions of the ICu16 sample, large metal particles are always obtained when the samples are calcined at 450 °C prior to reduction. This is especially striking for the sample dried at 25 °C that only contained small metal particles after direct reduction (Table 1). Besides, copper oxide particles are always formed during calcination of these samples, as shown by UV–visible spectroscopy (curves e–h of Figure 2B) and XRD. It is proposed that like during the drying step at 100 °C, calcination favors the coalescence and sintering of the Cu²⁺ species in the samples with high copper loading. So large CuO particles are formed, and large metal particles are obtained after reduction.

2. Formation of Copper Phyllosilicate. To our knowledge, this study is the first one that shows that copper phyllosilicate can form in Cu/SiO₂ samples prepared by cationic exchange with copper ammine complex. A more extensive study of the influence of the conditions of preparation⁵¹ shows that copper phyllosilicate is formed in solution during cationic exchange and that the amount of copper phyllosilicate increases with the copper concentration and the time of contact. It may be noted that the term “cationic exchange”, or “adsorption at equilibrium” also used in the literature, does not reflect chemical phenomena, which lead to the formation of phyllosilicates and involve a mechanism of dissolution–precipitation in solution. Silica-supported phyllosilicates are also known to be formed during preparations of Ni/SiO₂,^{4–8,52} Cu/SiO₂,²³ Zn/SiO₂,⁵³ and Co/SiO₂⁵⁴ by “cationic exchange” and/or deposition–precipitation. A molecular mechanism explaining the formation of supported nickel phyllosilicate during the preparation of Ni/SiO₂ by deposition–precipitation has been proposed.³ It is based on the dissolution of silica in basic medium and the reprecipitation of phyllosilicates. The silicic acid released in solution can react with metal complexes containing bridging ligands such as H₂O or OH. Condensation reactions of ololation-type lead to Si–OH–Ni bridges, then to polymerization of phyllosilicate on the silica surface.

As mentioned in the Introduction, Kohler et al.¹⁹ reported the size of copper metal particles in Cu/SiO₂ samples prepared by cationic exchange with [Cu(NH₃)₄(H₂O)₂]²⁺. After calcination at 280 °C and reduction up to 350 °C, the average size of

metal particles was 10 to 20–40 Å for Cu loadings between 2.1 and 9.5 wt % Cu. The authors noted the presence of nonfully reduced Cu⁺ ions in their samples. To explain their results, they proposed that (i) after drying, the catalysts contain two types of copper species, grafted–isolated Cu²⁺ ions and Cu(OH)₂, the latter arising from precipitation during the washing step, (ii) during calcination, Cu(OH)₂ transforms into CuO particles, and (iii) during reduction, the CuO particles are reduced to Cu⁰ particles while the grafted–isolated Cu²⁺ ions are reduced to Cu⁺. Our experiments give different results: (i) no Cu⁺ is detected by photoluminescence after reduction probably because of the higher temperature of reduction; (ii) the presence of copper phyllosilicate is detected. We suggest that the Cu(OH)₂ that Kohler et al. proposed to be at the origin of the formation of CuO, and then of metal particles, is in fact the copper phyllosilicate. This point will be fully developed in ref 51.

As mentioned above, copper phyllosilicate is not detected in the ECu_{en} sample, although it has also been prepared under basic conditions. This is also true for Ni/SiO₂ samples prepared by cationic exchange with [Ni(en)₃]²⁺^{8,55} and [Ni(en)₂(H₂O)₂]²⁺.⁵⁶ This is explained by the fact that ethanediamine is a nonbridging and a strong chelating ligand, so reaction by condensation with silicic acid cannot occur.¹

3. Influence of the Strength of the Precursor–Support Interaction on the Metal Particle Size. The different average sizes of metal particles obtained for the different Cu/SiO₂ samples studied here may be related to different metal–support interactions. Different Cu²⁺–silica interactions are established during the preparations in solution and the thermal treatments. As regard the Cu/SiO₂ samples prepared by “cationic exchange”, it seems that the Cu²⁺ species has to be chemically bonded to the silica support to lead to small metal particles. Indeed, when the ECu_{en} sample is reduced just after drying, the Cu²⁺ species, which were in electrostatic interaction with the silica support after drying, give large metal particles (Table 2). In contrast, when the sample is reduced after calcination, the Cu²⁺ ions, which were grafted on the silica surface, lead to small metal particles. In the case of the ECu_{am} sample, the Cu²⁺ ions are grafted on the silica surface or involved in a copper phyllosilicate (Figure 3) whether the sample is dried or calcined. In both cases, small metal particles are generated. Hence, the key step to obtain small metal particles in samples prepared by “cationic exchange”, i.e., to avoid sintering during reduction, is the establishment of chemical bonds between Cu²⁺ and silica or silicate layers before reduction. This is in agreement with the conclusions drawn by Bruce et al.⁵⁷ and by van der Oetelaar et al.⁵⁸ in their studies of model Cu/SiO₂ catalysts. Chemical bonds are formed during drying at 25 °C for the ECu_{am} samples and during calcination for the ECu_{en} sample.⁴⁸ Geus et al.²³ also showed the presence of copper phyllosilicate in Cu/SiO₂ materials prepared by deposition–precipitation, and the average size of metal particles was small too, from 23–27 Å (5 wt % Cu) to 61–82 Å (34 wt % Cu). The grafting of Cu²⁺ on the silica surface and the presence of copper phyllosilicate are not the only conditions for obtaining small metal particles. Small metal particles are also formed in the ICu samples dried at 25 °C, although Cu²⁺ is not bonded to the silica support. Indeed, a mere washing with water leaches all the supported copper nitrate. The reason that the metal particles are small in the ICu samples dried at 25 °C is not fully explained. However, it seems to be related to the fact that after drying at 25 °C, the supported copper is a hydrated nitrate spread on the silica surface while after drying at 100 °C, it agglomerates as a dehydrated nitrate hydroxide.

4. Comparison with the Ni/SiO₂ Materials. The results obtained here with Cu/SiO₂ samples can be compared to those previously obtained on Ni/SiO₂ samples. In contrast to the dried ECu_{en} samples, which give large metal particles after reduction (Table 2), dried Ni/SiO₂ samples prepared by cationic exchange with nickel tris-ethanediamine give small metal particles (~20 Å).^{8,59,60} The formation of these small nickel metal particles was related to the ability of the metal nickel to catalyze the reaction of hydrogenolysis of amines.⁶¹ It was proposed that the hydrogenolysis of the ethanediamine ligands led to the grafting of Ni²⁺ on silica and simultaneously to the nickel reduction.^{59,60} Since Cu⁰ is much less active than nickel in the reactions of hydrogenolysis,⁶² hydrogenolysis of ethanediamine does not take place during the reduction of the ECu_{en} sample, so the Cu complexes do not graft onto silica and, as a consequence, the metal particles are larger.

If one considers the most favorable thermal pretreatment for obtaining small metal particles in ICu samples, i.e., drying at 25 °C, the metal particles (~30 Å in ICu4 and ICu16 (Table 1)) are as small as those of Cu/SiO₂ samples prepared by cationic exchange or even smaller (Table 2). This result is quite unusual, since samples prepared by impregnation are known to lead to significantly larger metal particles than samples prepared by ion exchange. In the case of Ni/SiO₂, average sizes of 20–30 Å are obtained by cationic exchange⁸ whereas average sizes of 60–70 Å are obtained by impregnation.⁴⁹ Another difference between the two systems is that in impregnated Ni/SiO₂ samples, the size of the metal particles does not depend on the drying conditions; whether they are dried at 25 or 90 °C for up to 170 h, they give the same average size of particles (60–70 Å) after TPR up to 700 °C, although nitrate hydroxide is also formed during drying at 90 °C.⁴⁹ The constant size of the metal particles in Ni/SiO₂ samples was attributed to the formation of nickel phyllosilicates during the drying step at 90 °C and during the TPR heating ramp before the beginning of the process of reduction. These nickel phyllosilicates would be located at the metal–support interface and would act as anchoring sites for the remaining nickel. In the ICu samples, copper phyllosilicate has not been detected.

Conclusion

A systematic study of the size of copper metal particles supported on silica as a function of the preparation route and thermal treatments has been carried out. The copper species formed after drying and calcination have been characterized. Several new features have been pointed out.

(1) The classical incipient wetness impregnation method may lead to metal particles (~30 Å) as small as in samples prepared by cationic exchange, and not to a bimodal distribution of sizes with a population of large particles as reported in refs 9 and 10, at least provided that the drying step is performed at room temperature. It is shown that the drying step, so often neglected in the literature, has a drastic influence on the size of the metal particles even though calcination and reduction are performed at much higher temperature.

(2) For the samples prepared by cationic exchange, the establishment of chemical Cu²⁺–silica bonds is the key step for the obtention of small metal particles. This chemical bonding is established during drying for the samples prepared from the [Cu(NH₃)₄(H₂O)₂]²⁺ precursor and during calcination for the samples prepared from the [Cu(en)₂(H₂O)₂]²⁺ precursor.

(3) The formation of copper phyllosilicate is for the first time pointed out in Cu/SiO₂ samples prepared by cationic exchange. It is formed in solution according to a mechanism of silica

dissolution–silicate precipitation, the formation of silicate depending on the nature of the ligands (bridging or nonbridging) in the coordination sphere of the metal complexes.

Acknowledgment. The students, S. Allier, C. Chouillet, and B. Dewynter are acknowledged for having made additional experiments during their short period in the laboratory. B. Morin and M. Lavergne are thanked for their technical assistance in ESR spectroscopy and electron microscopy, respectively. A. Decarreau is acknowledged for providing us with bulk chrysocolla.

References and Notes

- (1) Che, M. *Studies in Surface Science and Catalysis*; Guzzi, L., Solymosi, F., Tetenyi, P., Eds.; Elsevier: Amsterdam, 1993; Vol. 75A, p 31.
- (2) Lambert, J. F.; Che, M. In *Dynamics of Surfaces and Reaction Kinetics in Heterogeneous Catalysis*; Froment, G. F., Waugh, K. C., Eds.; Elsevier: Amsterdam, 1997; p 91.
- (3) Burattin, P.; Che, M.; Louis, C. *J. Phys. Chem. B* **1998**, *102*, 2722.
- (4) van Dillen, J. A.; Geus, J. W.; Hermans, L. A.; van der Meijden, J. *Proc. Int. Congr. Catal.*, 6th **1977**, 677.
- (5) Burattin, P.; Che, M.; Louis, C. *J. Phys. Chem. B* **1997**, *101*, 7060.
- (6) Clause, O.; Kermarec, M.; Bonneviot, L.; Villain, F.; Che, M. *J. Am. Chem. Soc.* **1992**, *114*, 4709.
- (7) Kermarec, M.; Carriat, J. Y.; Burattin, P.; Che, M.; Decarreau, A. *J. Phys. Chem.* **1994**, *98*, 12008.
- (8) Che, M.; Cheng, Z. X.; Louis, C. *J. Am. Chem. Soc.* **1995**, *117*, 2008.
- (9) Jackson, S. D.; Robertson, F. J.; Willis, J. *J. Mol. Catal.* **1990**, *63*, 255.
- (10) Kuijpers, E. G. M.; Tjepkema, R. B.; Van der Wal, W. J. J.; Mesters, C. M. A. M.; Spronck, S. F. G. M.; Geus, J. W. *Appl. Catal.* **1986**, *25*, 139.
- (11) Kakuta, N.; Kazusaka, A.; Yamazaki, A.; Miyahara, K. *J. Chem. Soc., Faraday Trans. 1* **1984**, *80*, 3245.
- (12) Millar, G. J.; Rochester, C. H.; Waugh, K. C. *J. Chem. Soc., Faraday Trans.* **1991**, *87*, 1467.
- (13) Padley, M. B.; Rochester, C. H.; Hutchings, G. J.; King, F. *J. Chem. Soc., Faraday Trans.* **1994**, *90*, 203.
- (14) Rouco, A. *J. Appl. Catal. A* **1994**, *117*, 139.
- (15) Tominaga, H.; Kaneko, M.; Ono, Y. *J. Catal.* **1977**, *50*, 400.
- (16) Shimokawabe, M.; Takezawa, N.; Kobayashi, H. *Appl. Catal.* **1982**, *2*, 379.
- (17) Monti, D.; Wainwright, M. S.; Trimm, D. L.; Cant, N. W. *Ind. Eng. Chem. Prod. Res. Dev.* **1985**, *24*, 397.
- (18) Kohler, M. A.; Lee, J. C.; Trimm, D. L.; Cant, N. W.; Wainwright, M. S. *Appl. Catal.* **1987**, *31*, 309.
- (19) Kohler, M. A.; Curry-Hyde, H. E.; Hughes, A. E.; Sexton, B. A.; Cant, N. W. *J. Catal.* **1987**, *108*, 323.
- (20) Clause, O.; Bonneviot, L.; Che, M.; Verdager, M.; Villain, F.; Bazin, D.; Dexpert, H. *J. Chim. Phys.* **1989**, *86*, 1767.
- (21) Kenvin, J. C.; White, M. G.; Mitchell, M. B. *Langmuir* **1991**, *7*, 1198.
- (22) Kenvin, J. C.; White, M. G. *J. Catal.* **1991**, *130*, 447.
- (23) Van der Grift, C. J. G.; Elberse, P. A.; Mulder, A.; Geus, J. W. *Appl. Catal.* **1990**, *59*, 275.
- (24) van de Scheur, F. T.; van der Linden, B.; Mittelmeijer-Hazeleger, M. C.; Nazlloomian, J. G.; Staal, L. H. *Appl. Catal. A* **1994**, *111*, 63.
- (25) Brands, D. S.; Poels, E. K.; Blick, A. *Appl. Catal. A* **1999**, *184*, 279.
- (26) Taghavi, M. B.; Pajonk, G.; Teichner, S. J. *Bull. Soc. Chim. Fr.* **1978**, 1-302.
- (27) Stambach, M. R.; Thomas, D. J.; Trimm, D. L.; Wainwright, M. S. *Appl. Catal.* **1990**, *58*, 209.
- (28) Wehrli, J. T.; Thomas, D. J.; Wainwright, M. S.; Trimm, D. L.; Cant, N. W. *Appl. Catal.* **1990**, *66*, 199.
- (29) Wehrli, J. T.; Thomas, D. J.; Wainwright, M. S.; Trimm, D. L.; Cant, N. W. *Appl. Catal.* **1991**, *70*, 253.
- (30) Koeppe, R. A.; Wehrli, J. T.; Wainwright, M. S.; Trimm, D. L.; Cant, N. W. *Appl. Catal. A* **1994**, *120*, 163.
- (31) Ossipoff, N. J.; Cant, N. W. *J. Catal.* **1994**, *148*, 125.
- (32) Chambers, A.; Jackson, S. D.; Stirling, D.; Webb, G. *J. Catal.* **1997**, *168*, 301.
- (33) Robbins, J. L.; Iglesia, E.; Kelkar, C. P.; de Rites, B. *Catal. Lett.* **1991**, *10*, 1.
- (34) Sodesawa, T. *React. Kinet. Catal. Lett.* **1984**, *24*, 259.
- (35) Ai, M. *Appl. Catal.* **1984**, *11*, 259.
- (36) Guerreiro-Ruiz, A.; Rodriguez-Ramoz, I.; Fierro, J. L. G. *Appl. Catal.* **1991**, *72*, 119.
- (37) Marchi, A. J.; Fierro, J. L. G.; Santamaria, J.; Monzon, A. *Appl. Catal. A* **1996**, *142*, 375.
- (38) Guerreiro, E. D.; Gorris, O. F.; Rivarola, J. B.; Arrua, L. A. *Appl. Catal. A* **1997**, *165*, 259.
- (39) Evans, J. W.; Casey, P. S.; Wainwright, M. S.; Trimm, D. L.; Cant, N. W. *Appl. Catal.* **1983**, *7*, 31.
- (40) Decarreau, A. *Geochim. Cosmochim. Acta* **1985**, *49*, 1537.
- (41) Boreskov, G. K. *Proc. Int. Congr. Catal.*, 6th **1976**, 204.
- (42) Surin, S. A.; Shelimov, B. N.; Mikheikin, I. D.; Kazanskii, V. B. *Kinet. Catal.* **1976**, *17*, 1569.
- (43) Hathaway, B. J. In *Comprehensive Coordination Chemistry, The Synthesis, Reactions & Applications of Coordination Compounds*; Wilkinson, G., Gillard, R. D., McCleverty, J. A., Eds.; Pergamon Press: Oxford, 1987; Vol. 5, p 669.
- (44) Friedman, R. M.; Freeman, J. J.; Lytle, F. W. *J. Catal.* **1978**, *55*, 10.
- (45) Marion, M. C.; Garbowski, E.; Primet, M. *J. Chem. Soc., Faraday Trans.* **1990**, *86*, 3027.
- (46) Chukhrov, F. V.; Zvyagin, B. B.; Ermilova, L. P.; Gorshov, A. I.; Rudnitskaya, E. S. *Proc. Int. Clay. Conf.* **1969**, *1*, 141.
- (47) Van Oosterwyck-Gastuche, M. C. *C. R. Acad. Sci.* **1970**, D271, 1837.
- (48) Trouillet, L.; Toupance, T.; Villain, F.; Louis, C. *Phys. Chem. Chem. Phys.*, submitted.
- (49) Louis, C.; Cheng, Z. X.; Che, M. *J. Phys. Chem.* **1993**, *97*, 5703.
- (50) Delmon, B. In *Handbook on Heterogeneous Catalysis*; Ertl, G., Knözinger, H., Weitkamp, J., Eds.; VCH: Weinheim, 1997; Vol. 1, p 264.
- (51) Toupance, T.; Kermarec, M.; Louis, C. To be published.
- (52) Hermans, L. A. M.; Geus, J. W. In *Preparation of Catalysts II*; Delmon, B., Grange, P., Jacobs, P. A., Poncelet, G., Eds.; Elsevier: Amsterdam, 1979; p 113.
- (53) Chouillet, C.; Pernot, H.; Kermarec, M.; Louis, C. Unpublished results.
- (54) Trujillano, R.; Grimoult, J.; Lambert, J. F.; Louis, C. *Proc. Int. Congr. Catal.*, 12th, in press.
- (55) Bonneviot, L.; Clause, O.; Che, M.; Manceau, A.; Dexpert, H. *Catal. Today* **1989**, *6*, 39.
- (56) Lambert, J. F.; Hoogland, M.; Che, M. *J. Phys. Chem. B* **1997**, *101*, 10347.
- (57) Bruce, D.; Aaron Bertrand, J.; White, M. G. *AIChE J.* **1993**, *39*, 1966.
- (58) van der Oetelaar, L. C. A.; Partridge, A.; Toussaint, S. L. G.; Flipse, C. F. J.; Brongersma, H. H. *J. Phys. Chem. B* **1998**, *102*, 9541.
- (59) Cheng, Z. X.; Louis, C.; Che, M. *Stud. Surf. Sci. Catal.* **1993**, *89*, 1785.
- (60) Cheng, Z. X.; Louis, C.; Che, M. *Stud. Surf. Sci. Catal.* **1995**, *91*, 1027.
- (61) Sabatier, P.; Gaudion, G. *C. R. Acad. Sci. Fr.* **1915**, *9*, 165.
- (62) Sinfelt, J. H. *Adv. Catal.* **1973**, *23*, 91.